Role of tropical Pacific SSTs in global medieval hydroclimate: A modeling study

Robert Burgman,[1] Richard Seager,[2] Amy Clement,[1] and Celine Herweijer[3]

Received 18 December 2009; revised 20 January 2010; accepted 17 February 2010; published 19 March 2010.

[1] The role of tropical Pacific SSTs in driving global medieval hydroclimate is assessed. Using fossil coral records from Palmyra Atoll, tropical Pacific sea surface temperature (SST) boundary conditions are derived for the period 1320–1462 A.D. These boundary conditions consist of La Niña-like mean state conditions in the tropical Pacific with inter-annual and decadal variability about that altered state. The reconstructed SSTs in the tropical Pacific are used to force a 16 member ensemble of atmospheric general circulation model (AGCM) simulations, coupled to a one layer ocean model outside of the tropical Pacific. The AGCM simulations of medieval climate are compared with modern climate simulations for the period 1856–2005 A.D. and are shown to reproduce many aspects of medieval hydroclimate found in paleo-proxy records for much of the Western Hemisphere, northern Eurasia, and the northern tropics. These results suggest that many features of global medieval hydroclimate changes can be explained by changes in tropical Pacific SSTs, though the potential role for other oceans is also discussed. **Citation:** Burgman, R., R. Seager, A. Clement, and C. Herweijer (2010), Role of tropical Pacific SSTs in global medieval hydroclimate: A modeling study, *Geophys. Res. Lett.*, *37*, L06705, doi:10.1029/2009GL042239.

1. Introduction

[2] Recent studies of the observational record as well as climate model studies point to North American drought variability being significantly controlled by SSTs in the tropical Pacific Ocean [*Seager et al.*, 2005a] with tropical Atlantic Ocean SSTs playing a supporting role. These studies show that during periods of prolonged (i.e. years to a decade) drought in the central US, tropical Pacific SSTs are anomalously cool. Multidecadal North American hydroclimate variability also appears influenced by multidecadal tropical Pacific SST anomalies [*Huang et al.*, 2005] that have the spatial structure of ENSO-like Pacific decadal variability (PDV) [*Zhang et al.*, 1997; *Burgman et al.*, 2008a]. While several potential mechanisms for this pattern of variability in the Pacific can be found in the literature [*Burgman et al.*, 2008b; *Clement et al.*, 2009], the origin of PDV remains unclear.

[3] Recent research suggests that decadal variability in precipitation in North America and remote regions of the world is similar to that seen on interannual timescales associated with ENSO [*Seager et al.*, 2003]. When La Niña-like SST patterns persist for a period of years, model studies have shown that they provide a steady atmospheric forcing necessary for drying in the subtropics associated with poleward shifts in the subtropical jets [*Seager et al.*, 2005a; *Herweijer et al.*, 2006]. This response is a low frequency realization of the Tropical Modulation of Mid-latitude Eddies (TMME mechanism), which operates on seasonal to inter-annual time-scales [*Seager et al.*, 2005b]. The zonally and hemispherically symmetric nature of the TMME, suggests that drought in North America may coincide with hydroclimate changes in other regions. *Herweijer et al.* [2006] and *Seager et al.* [2007] have shown that areas of central and southern South America as well as central and Eastern Europe have experienced severe drought coincident with droughts in North America. This in-phase relationship suggests persistent La Niña-like tropical Pacific SSTs can have a global impact.

[4] For the western US, paleo-reconstructions of drought conditions indicate that the droughts of the last 150 years are considerably less severe and protracted than those that have been estimated for time periods in the 12th and 13th century from tree ring data [*Woodhouse and Overpeck*, 1998]. *Herweijer et al.* [2007] and *Seager et al.* [2007] analyzed a recently updated reconstruction of North American drought [*Cook and Krusic*, 2004; *Cook et al.*, 2004] dating back to 1A.D. as well as oceanic proxy data to conclude that tropical SSTs during the extended "mega-droughts" of the Medieval Climate Anomaly (MCA, defined here as the period between 800A.D and 1500 A.D.) were consistent with a La Niña-like PDV pattern of SST. A similar conclusion was reached by *Graham et al.* [2007]. However, *Seager et al.* [2007] also suggested that changes in tropical Atlantic SSTs were needed to fully explain the North American and global medieval hydroclimate.

[5] The current research seeks to test the influence of persistent La Nina-like tropical Pacific SSTs alone in forcing medieval hydroclimate using a state of the art climate model. A detailed examination of the North American hydroclimatic response is discussed by *Seager et al.* [2008], and here we focus on the global response. A high-resolution paleo-proxy coral-based SST record from the central Pacific is used to reconstruct tropical Pacific SSTs for the period 1320–1462 A.D. The resulting SST reconstruction is used to force an ensemble of climate model simulations. Modeled estimates of medieval hydroclimate are compared to simulations forced by observed SSTs and the differences are verified using paleo-proxy records of medieval hydroclimate from around the world.

2. Paleo SST Reconstruction

[6] The procedure used to reconstruct tropical Pacific SST is described briefly here, but more details are provided by

[1]Rosenstiel School of Marine and Atmospheric Science, University of Miami, Miami, Florida, USA.
[2]Lamont-Doherty Earth Observatory, Earth Institute at Columbia University, Palisades, New York, USA.
[3]PricewaterhouseCoopers, LLP, London, UK.

0094-8276/10/2009GL042239

Seager et al. [2008]. To reconstruct tropical Pacific SSTs, we utilize high-resolution oxygen isotope data taken from fossil corals on Palmyra Atoll (6N, 160W) [*Cobb et al.*, 2003] and SST data from *Kaplan et al.* [1998]. We note that d18O measurements are sensitive to temperature and salinity, however, the analysis by *Cobb et al.* [2003] indicates that due to the tightly coupled nature of SST and precipitation in this region, the d18O records provide sensitive recorders of inter-annnual variability and mean climate change in the central tropical Pacific.

[7] Monthly SST and d18O anomalies are formed by removing the long-term monthly mean from each calendar month's mean value. To separate the interannual and lower frequency components of the d18O anomaly timeseries we applied a 6-year lowpass filter (as in work by *Zhang et al.* [1997]). The highpass filtered d18O is simply the unfiltered d18O anomalies minus the lowpass filtered anomalies. Multiple linear regression using least squares was then used to determine the spatial patterns of SST anomalies associated with high and low pass filtered d18O anomalies for modern observations. One result inherent to the least-squares regression process is that reconstructions have reduced variance relative to the original record. To address this issue we incorporate two indices used in the literature to describe inter-annual and decadal variability of SST. A lowpass filtered tropical Pacific index (20N–20S 160E–80W, from *Zhang et al.* [1997] and the highpass filtered NIÑO34 index (170W–120W, 5S–5N). To inflate the variance of the reconstructed SST components we normalized these reconstructed indices by their standard deviation to match the variance found in observations.

[8] The components of the modern SST reconstruction are modeled as

$$SST_{LP}(x,y,t) = \alpha(x,y)*d18O_{LP}(t)*N_{TPI}$$

$$SST_{HP}(x,y,t) = \beta(x,y)*d18O_{HP}(t)*N_{N34}$$

$$SST_{mod}(x,y,t) = SST_{climatology}(x,y,t) + SST_{LP}(x,y,t) + SST_{HP}(x,y,t)$$

Where $d18O_{LP/HP}$ is the lowpass/highpass filtered d18O anomaly derived from fossil coral data, α and β are the regression coefficients, and $N_{TPI/N34}$ is the constant used to normalize the lowpass/highpass variance. The medieval reconstruction is then:

$$SST_{LP14}(x,y,t) = \alpha(x,y)*(d18O_{LP14}(t) + \mu 14)*N_{TPI}$$

$$SST_{hP14}(x,y,t) = \beta(x,y)*d18O_{HP14}(t)*N_{N34}$$

$$SST_{14}(x,y,t) = SST_{climatology}(x,y,t) + SST_{LP14}(x,y,t) + SST_{HP14}(x,y,t)$$

Where $d18O_{LP14}$ and $d18O_{HP14}$ are the lowpass and highpass filtered d18O anomalies from the period 1320–1462 A.D. and $\mu 14$ is the difference in the long-term climatological mean from the modern d18O record. Due to the paucity of data describing ocean temperatures and circulation for the period 1320–1462 A.D. we can do little more than assume that the spatial patterns of ENSO and PDV (regression coefficients α and β) were the same in the Medieval period as in the modern period. Of course it is possible that changes in the in the mean state of the ocean, induced by changes in circulation for example, could lead to different spatial structures of the dominant modes of variability. However, in the absence of information on past changes in the ocean state, we necessarily ignore this possibility. Additionally, the variance adjustment of reconstructed SSTs will introduce some error in the reconstructed SSTs. We note that the difference between the reconstructed mean state and modern SSTs is an order of magnitude smaller than seen in similar studies [*Graham et al.*, 2007] but of comparable magnitude to the SST anomalies that forced multiyear droughts in the historical period [*Seager et al.*, 2005a].

3. Model

[9] The AGCM used for this experiment is the National Center for Atmospheric Research (NCAR) Community Climate Model 3 (CCM3) run at T42 resolution with 18 vertical levels [*Kiehl and Gent*, 2004]. Previous studies have shown that this model is capable of simulating 19th and 20th Century droughts within the instrumental period [*Seager et al.*, 2005a; *Herweijer et al.*, 2006]. The model simulations analyzed in the current study include a 16-member ensemble from 1856 to 2005, each with different initial conditions, forced with observed global SSTs. This is the Global Ocean Global Atmosphere (GOGA) ensemble.

[10] The second simulation is a 16-member ensemble forced by the reconstructed tropical Pacific SSTs (20°S–20°N), for the period 1320 to 1462 A.D., coupled to a uniform 75m deep mixed layer ocean elsewhere. The mixed layer ocean contains a specified seasonally varying heat flux correction, or q-flux, that parameterizes the effects of ocean heat transport convergence (i.e. horizontal advection by ocean currents, upwelling, and the deepening and shoaling of the mixed layer depth) and minimizes modeled surface flux errors. The POGA-1L q-flux ensures that the computed SST, when run with modern SSTs in the tropical Pacific, remains close to the modern climatology. Departures of the SST outside of the tropical Pacific from modern climatology are due to the influence of these specified medieval tropical Pacific SSTs communicated through the atmosphere and into the ocean by surface fluxes. This is the Pacific Ocean Global Atmosphere - 1 Layer mixed layer model outside of the Pacific (POGA-1L) ensemble. The 16-member ensemble means are used in the analysis of atmospheric and land surface output.

[11] While there is a clear difference in experimental design of the GOGA and POGA-lL model simulations, the use of simulations that allow time-varying modern estimates of SSTs in a particular basin have been used effectively as diagnostic tools. Previous studies by *Seager et al.* [2005a] and *Herweijer et al.* [2006] have shown that Pacific Ocean forced AGCMs have been successful at reproducing modern persistent drought. The current study, therefore, builds on previous studies by simulating tropical Pacific forced climate using estimates of SST from paleoclimatic records. We do not intend to suggest that SST anomalies not generated within, or remotely forced by, the tropical Pacific were unimportant to medieval hydroclimate but faced with the limited availability of proxy SST reconstructions, here merely attempt to isolate the tropical Pacific impact. A

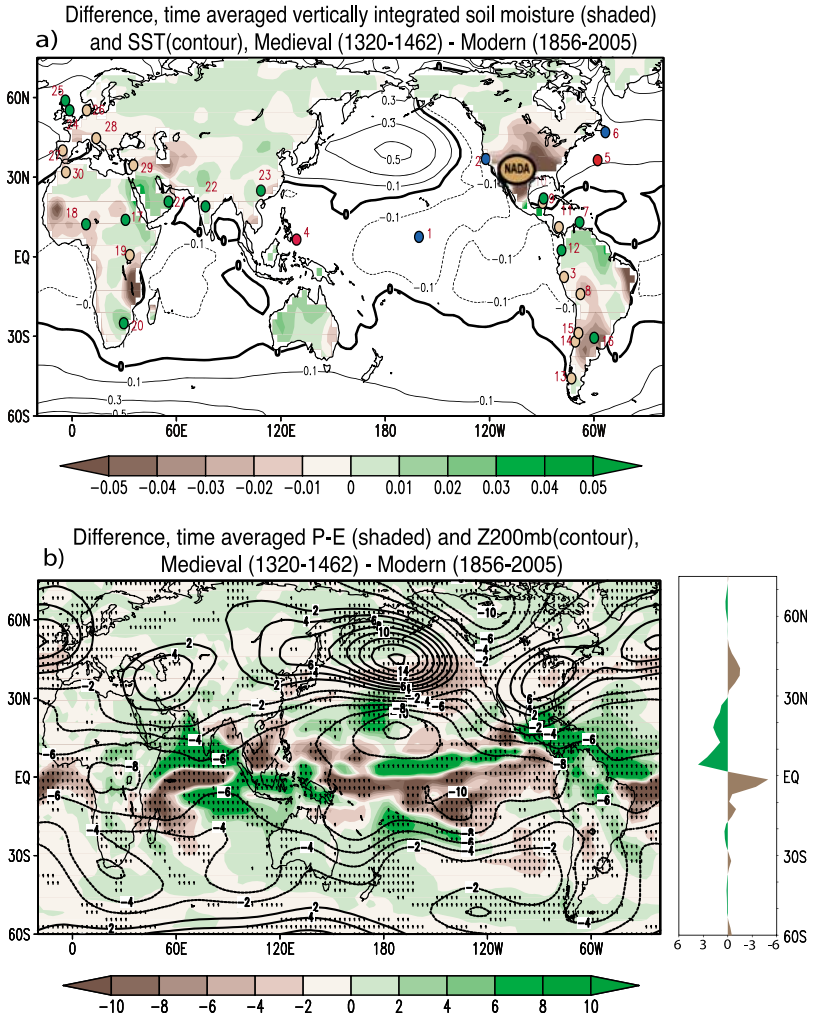

Figure 1. (a) Long term mean differences of vertically integrated soil wetness (shaded, (mm^3H2O)/(mm^3soil)) and SST (contour, 0.10 C) between POGA-1L (1320–1462 A.D.) and GOGA simulation (1856–2005 A.D.) overlaid with records of medieval hydroclimate and SST. SST records are plotted as red (warm) or blue (cool) dots relative to modern observations. Green and brown dots indicate proxy records of wet or dry medieval hydroclimate. The numbers cross-reference the records to the references in the text and Table S1 (see auxiliary material). The medieval period is taken to be, approximately, from 800 A.D. to 1500 (adapted from *Seager et al.* [2007]). (b) The long term mean difference in Precipitation minus Evaporation (P-E is shaded, units are mm/month, significance levels of 95% stippled) and 200mb geopotential height (contours, units are meters) for the winter half year between the POGA-1L simulation (1320–1462 A.D.) and the modern GOGA simulation (1886–1998A.D.). The difference in the zonal average P-E is offset to the right.

discussion of the limitations of this experimental design is provided in the next section.

4. Model Simulated Medieval Hydroclimate

[12] Here we analyze differences in the mean hydroclimate between the modern GOGA and medieval POGA-1L simulations and assess whether these changes are consistent with the global pattern of hydroclimate change found in paleo-proxy records. Modeled anomalies are calculated as differences between ensemble means for the period 1320A.D.–1462 A.D. of the POGA-1L simulation and the period 1856A.D.–2005 A.D. of the GOGA simulation. Additional analysis was performed on a modern POGA simulation with historical SSTs specified in the tropical Pacific and climatological SSTs specified elsewhere and the computed differences were qualitatively similar.

[13] Figure 1a shows the difference in the long-term mean soil moisture (shaded) and SST (contours) with the estimates from the paleo-proxy records displayed as colored circles. The colored circles illustrate the SST and hydroclimate conditions of the MCA with respect to modern observations as described by available paleo-proxy data from around the world (adapted from *Seager et al.* [2007]). Red (blue) dots represent warmer (cooler) SSTs while green (tan) dots represent wetter (dryer) conditions. The numbers by the dots correspond to those in Table S1 (see auxiliary material).[1] The specifics of these records and their limita-

[1] Auxiliary materials are available in the HTML. doi:10.1029/2009GL042239.

tions are covered in some detail by *Herweijer et al.* [2007] and *Seager et al.* [2007] and, for some, also by *Graham et al.* [2007]. In order to compare modeled hydroclimate to the various paleo-proxy records we analyze the difference in model simulated vertically integrated soil wetness of the root zone (top 0.7 meters), which is significantly correlated with PDSI in observations [*Dai et al.*, 2004].

[14] The differing natures of the various proxy reconstructions of hydroclimate, varying from tree rings to flood records, do not allow a quantitative comparison with the model simulation. Instead we are looking for a one sided agreement: conditions either wetter or drier than modern conditions consistently through the medieval period.

[15] The imposed SST in the tropical Pacific (Figure 1a) is a La-Niña-like PDV pattern of comparable amplitude to that associated with modern persistent droughts [*Seager et al.*, 2007]. The east-west gradient of SST in the western (4) and central (1) near-equatorial Pacific is in qualitative agreement with the d18O analysis of *Cobb et al.* [2003] and a Mg/Ca analysis of a marine sediment core near the island of Mindanao [*Stott et al.*, 2004], though the latter record indicates a warming that is not supported by our SST reconstruction. Outside the tropical Pacific the model ocean mixed layer responds to surface fluxes forced from the tropical Pacific with cooling throughout the global tropics and warming in the extra-tropical Pacific and Atlantic, though the paleo-proxy records are not in agreement in the North Atlantic (5,6) where *Seager et al.* [2007] suggest a positive Atlantic Multidecadal Oscillation (AMO) played a significant role in medieval climate.

[16] In North America, the strong negative values of soil wetness are consistent with high resolution tree ring records from the North American Drought Atlas (NADA) of *Cook et al.* [2004] and *Cook and Krusic* [2004], which indicate that much of the Southwest and the Great Plains region were drier during the MCA than in the Little Ice Age and modern times. The North American response is examined in more detail by *Seager et al.* [2008]. These warm, dry conditions extend across the Atlantic to Europe and N.W. Africa where historical lake level records (28), river flood records (26, 27) and tree ring data (30) indicate more arid conditions. Dry conditions extend through continental Europe and as far east as central Asia and the Middle East, where a high-resolution speleothem record from Israel (29) indicates more arid conditions. Further north the wet conditions captured by a high-resolution speleothem record in Scotland (25) are not simulated in the model though a zonal pattern of increased soil moisture in the high northern latitudes is evident, as reflected in the zonal mean precipitation minus evaporation (Figure 1b).

[17] The atmospheric response to the imposed La Niña-like mean state in the northern mid-latitudes is similar to that operating on decadal time-scales [*Seager et al.*, 2007]. Figure 1b shows the anomalous mean state precipitation minus evaporation (P-E) and 200mb geopotential heights for the medieval POGA-1L simulation relative to the modern GOGA simulation. In the POGA-1L simulation, La Niña-like cooling in the tropics causes a northward shift in the zonal mean position of the subtropical jet and associated transient eddies (not shown). This poleward shift in transient eddies leads to increased meridional eddy momentum flux convergence in the subtropics, an induced poleward flow, and increased subsidence and drying in the midlatitudes. The tropical Pacific forced shifts in transient eddies are communicated as far east as the Atlantic Ocean and Europe, consistent with the 200mb geopotential heights seen in Figure 1b [*Seager et al.*, 2003, 2005b].

[18] In a series of recent studies *Haug et al.* [2001] and *Peterson and Haug* [2006] suggest that during warm interstadials and periods of Holocene and deglacial warmth there is a northward shift in the position of the Atlantic ITCZ. Figure 1b shows that such a shift can be driven by a La Nina-like state in the tropical Pacific via cooler mean SSTs in the tropical South Atlantic and North Atlantic warming (shown in Figure 1a). This mechanism differs from previous studies that suggest shifts in the ITCZ are associated with internal Atlantic dynamics [*Zhang and Delworth*, 2005; *Mantsis and Clement*, 2009]. Wet conditions in central and northern South America shown in Figure 1a, are consistent with titanium concentrations in the Cariaco Basin (7) that measure the strength of river flow from northern South America. In the Yucatan peninsula, *Hodell et al.* [2005] (10) find a transition to a drier climate in the 15th century consistent with a wetter medieval climate simulated by the model. However, it should be noted that they also provide evidence for a series of decadal scale droughts between 900 and 1100 A.D. (9). In Ecuador (12), clastic sedimentation rates suggest relatively high precipitation while a high-resolution speleothem in Panama (11) finds a decrease in precipitation. The Ecuador record is consistent with wetter conditions there in the model, probably forced by cooling of the tropical Pacific Ocean.

[19] The out of phase relationship between the Cariaco Ti record (7) and the oxygen isotope content of ice in the Quelccaya ice cap (8) discussed by *Peterson and Haug* [2006] is also simulated in the POGA-1L model run. These more arid South American conditions extend south to the Patagonia region of Argentina and are consistent with analyses of tree rings (14), lake sediments (15) and relic tree stumps (13) dated to the medieval period. On the eastern side of the Andes, however, several studies of landforms, soils and archaeological remains (16) find consistent evidence of wet conditions not seen in the POGA-1L simulation.

[20] In the eastern equatorial Atlantic, the POGA-1L model simulates dry conditions in the Sahel and the Gulf of Guinea coastal regions. As with Northeast Brazil, precipitation in these regions is influenced by tropical Atlantic SSTs as well as by Pacific SSTs. While paleo-proxy records are sparse in these regions, evidence from ostracod faunal assemblages and shell chemistry, sediment properties, and palynology point to wetter conditions in the West African Sahel, which receives most of its rainfall when the ITCZ migrates northwards (18). This model-data inconsistency suggests that SST variability in the Atlantic involved ocean dynamics either remotely forced from the Pacific [e.g., *Latif and Grotzner*, 2000], or internal to the Atlantic Ocean as suggested by *Seager et al.* [2007], that likely played an important role in the hydroclimate of the MCA around the Atlantic basin.

[21] Wetter modeled conditions simulated in the northern tropics from Ethiopia (17) through the Arabian peninsula (21), India (22), and China (23), are in broad agreement with

proxy records there suggesting a stronger Asian monsoon during Medieval times. Simulated dry conditions in equatorial East Africa are consistent with several records of lake levels (19) from the MCA and are supported by the results of *Peterson and Haug* [2006] who show obvious co-variation between Cariaco Ti and Lake Malawi silica levels throughout the Holocene. In Australia, where records are sparse, the wetter conditions simulated in the POGA-1L simulations cannot be verified for this period. However, the SSTs shown in Figure 1a are consistent with a persistent weak negative phase of the Indian Ocean Dipole (IOD). Such events are associated with wetter than normal conditions in East Asia, Australia, and the Arabian Peninsula, and drought in parts of India and East Africa [*Saji et al.*, 1999; *Meyers et al.*, 2007, *Ummenhofer et al.*, 2009].

5. Discussion and Conclusions

[22] We have used a coral-based tropical Pacific SST field for the period 1320–1462 A.D. to force an ensemble of AGCM simulations. The coral based SSTs are characterized by a La Niña-like basic state in the tropical Pacific with variability on inter-annual to inter-decadal timescales. The model response to these conditions is similar to that seen in the observational record and model studies of modern persistent drought. La Niña-like SSTs in the tropical Pacific force a poleward shift in the northern hemisphere transient eddies leading to increased subsidence and drying in the northern subtropics and midlatitudes as far east as the European continent. Increased precipitation in the northern tropics, with the exception of West Africa, is associated with a strengthening of the monsoons in Asia and Central America. The hydrological changes simulated by the POGA-1L model for the medieval period are in agreement with paleo-proxy records from this period for much of the Western Hemisphere, northern Eurasia, and the northern tropics. The regions where the model-data intercomparison fails (e.g. tropical West Africa, Scotland) are regions that are influenced by Atlantic SSTs and the North Atlantic Oscillation (NAO). *Seager et al.* [2007] suggest that positive phases of the AMO and NAO likely played important roles in explaining the hydroclimate records for many such regions of the globe that are only influenced by the tropical Pacific. As such, tropical Pacific SST anomalies were an important forcing agent of Medieval hydroclimate anomalies but cannot fully explain the reconstructed pattern.

References

Burgman, R. J., A. C. Clement, C. Mitas, J. Chen, and K. Esslinger (2008a), Evidence for atmospheric feedbacks in the subtropical Pacific on decadal timescales, *Geophys. Res. Lett.*, *35*, L01704, doi:10.1029/2007GL031830.

Burgman, R. J., P. S. Schopf, and B. P. Kirtman (2008b), Decadal modulation of ENSO in a hybrid coupled model, *J. Clim.*, *21*, 5482–5500, doi:10.1175/2008JCLI1933.1.

Clement, A. C., R. J. Burgman, and J. R. Norris (2009), Observational and model evidence for positive low-level cloud feedback, *Science*, *325*, 460–464, doi:10.1126/science.1171255.

Cobb, K., C. D. Charles, H. Cheng, and R. L. Edwards (2003), El Nino/Southern Oscillation and tropical Pacific climate during the last millennium, *Nature*, *424*, 271–276, doi:10.1038/nature01779.

Cook, E. R., and P. J. Krusic (2004), North American summer PDSI reconstructions, *Data Contrib. Ser. 2004-045*, World Data Cent. for Paleoclimatol., Boulder, Colo.

Cook, E. R., C. Woodhouse, C. M. Eakin, D. M. Meko, and D. W. Stahle (2004), Long term aridity changes in the western United States, *Science*, *306*, 1015–1018, doi:10.1126/science.1102586.

Dai, A., K. E. Trenberth, and T. Qian (2004), A global dataset of Palmer drought severity index for 1870–2002: Relationship with soil moisture and effects of surface warming, *J. Hydrometeorol.*, *5*, 1117–1130, doi:10.1175/JHM-386.1.

Graham, N., et al. (2007), Tropical Pacific-mid latitude teleconnections in medieval times, *Clim. Change*, *83*, 241285, doi:10.1007/s10584-007-9239-2.

Haug, G., K. A. Hughen, D. M. Sigman, L. C. Peterson, and U. Röhl (2001), Southward migration of the Intertropical Convergence Zone through the Holocene, *Science*, *293*(5533), 1304–1308, doi:10.1126/science.1059725.

Herweijer, C., R. Seager, and E. R. Cook (2006), North American droughts of the mid to late nineteenth Century: History, simulation and implications for medieval drought, *Holocene*, *16*, 159–171, doi:10.1191/0959683606hl917rp.

Herweijer, C., R. Seager, E. R. Cook, and J. Emile-Geay (2007), North American droughts of the last millennium from a gridded network of tree ring data, *J. Clim.*, *20*, 1353–1376, doi:10.1175/JCLI4042.1.

Hodell, D. A., M. Brenner, J. H. Curtis, R. Medina-Gonzalez, E. I.-C. Can, A. Albornaz-Pat, and T. P. Guilderson (2005), Climate change on the Yucatan peninsula during the Little Ice Age, *Quat. Res.*, *63*, 109–121, doi:10.1016/j.yqres.2004.11.004.

Huang, H.-P., R. Seager, and Y. Kushnir (2005), The 1976/77 transition in precipitation over the Americas and the influence of tropical sea surface temperature, *Clim. Dyn.*, *24*, 721–740, doi:10.1007/s00382-005-0015-6.

Kaplan, A., M. Cane, Y. Kushnir, A. Clement, M. Blumenthal, and B. Rajagopalan (1998), Analyses of global sea surface temperature 1856–1991, *J. Geophys. Res.*, *103*, 18,567–18,589, doi:10.1029/97JC01736.

Kiehl, J. T., and P. R. Gent (2004), The Community Climate System Model, version 2, *J. Clim.*, *17*, 3666–3682, doi:10.1175/1520-0442(2004)017<3666:TCCSMV>2.0.CO;2.

Latif, M., and A. Grotzner (2000), The equatorial Atlantic oscillation and its response to ENSO, *Clim. Dyn.*, *16*, 213–218, doi:10.1007/s003820050014.

Mantsis, D., and A. Clement (2009), Simulated variability in the mean atmospheric meridional circulation over the 20th century, *Geophys. Res. Lett.*, *36*, L06704, doi:10.1029/2008GL036741.

Meyers, G. A., P. C. McIntosh, L. Pigot, and M. J. Pook (2007), The years of El Niño, La Niña, and interactions with the tropical Indian Ocean, *J. Clim.*, *20*, 2872–2880, doi:10.1175/JCLI4152.1.

Peterson, L. C., and G. H. Haug (2006), Variability in the mean latitude of the Atlantic ITCZ as recorded by riverine input of sediments to the Cariaco Basin, *Palaeogeogr. Palaeoclimatol. Palaeoecol.*, *234*(1), 97–113, doi:10.1016/j.palaeo.2005.10.021.

Saji, N. H., B. N. Goswami, P. N. Vinayachandran, and T. Yamagata (1999), A dipole mode in the tropical Indian Ocean, *Nature*, *401*, 360–363.

Seager, R., N. Harnik, Y. Kushnir, W. Robinson, and J. Miller (2003), Mechanisms of hemispherically symmetric climate variability, *J. Clim.*, *16*, 2960–2978, doi:10.1175/1520-0442(2003)016<2960:MOHSCV>2.0.CO;2.

Seager, R., Y. Kushnir, C. Herweijer, N. Naik, and J. Velez (2005a), Modeling of tropical forcing of persistent droughts and pluvials over western North America: 1856–2000, *J. Clim.*, *18*, 4065–4088, doi:10.1175/JCLI3522.1.

Seager, R., N. Harnik, W. A. Robinson, Y. Kushnir, M. Ting, H. P. Huang, and J. Velez (2005b), Mechanisms of ENSO-forcing of hemispherically symmetric precipitation variability, *Q. J. R. Meteorol. Soc.*, *131*, 1501–1527, doi:10.1256/qj.04.96.

Seager, R., N. Graham, C. Herweijer, A. L. Gordon, Y. Kushnir, and E. Cook (2007), Blueprints for medieval hydroclimate, *Quat. Sci. Rev.*, *26*(19–21), 2322–2336, doi:10.1016/j.quascirev.2007.04.020.

Seager, R., R. Burgman, Y. Kushnir, A. Clement, E. Cook, N. Naik, and J. Miller (2008), Tropical Pacific forcing of North American medieval megadroughts: Testing the concept with an atmosphere model forced by coral-reconstructed SSTs, *J. Clim.*, *21*, 6175–6190, doi:10.1175/2008JCLI2170.1.

Stott, L., K. Cannariato, R. Thunell, G. H. Haug, A. Koutavos, and S. Lund (2004), Decline of surface temperature and salinity in the western tropical Pacific Ocean in the Holocene epoch, *Nature*, *431*, 56–59, doi:10.1038/nature02903.

Ummenhofer, C. C., M. H. England, P. C. McIntosh, G. A. Meyers, M. J. Pook, J. S. Risbey, S. G. Alexander, and A. S. Taschetto (2009), What causes southeast Australia's worst droughts?, *Geophys. Res. Lett.*, *36*, L04706, doi:10.1029/2008GL036801.

Woodhouse, C. A., and J. T. Overpeck (1998), 2000 years of drought variability in the central United States, *Bull. Am. Meteorol. Soc.*, *79*, 2693–2714, doi:10.1175/1520-0477(1998)079<2693:YODVIT>2.0.CO;2.

Zhang, R., and T. L. Delworth (2005), Simulated tropical response to a substantial weakening of the Atlantic thermohaline circulation, *J. Clim.*, *18*, 1853–1860, doi:10.1175/JCLI3460.1.

Zhang, Y., J. M. Wallace, and D. S. Battisti (1997), ENSO-like decade-to century scale variability: 1900–1993, *J. Clim.*, *10*, 1004–1020, doi:10.1175/1520-0442(1997)010<1004:ELIV>2.0.CO;2.

R. Burgman and A. Clement, Rosenstiel School of Marine and Atmospheric Science, University of Miami, 4600 Rickenbacker Causeway, Miami, FL 33149, USA. (rburgman@rsmas.miami.edu)

C. Herweijer, PricewaterhouseCoopers, LLP, 1 Embankment Pl., London WC2N 6RH, UK.

R. Seager, Lamont-Doherty Earth Observatory, Earth Institute at Columbia University, Route 9W, Palisades, NY 10964, USA.